

# Experimental Demonstration of Femtosecond Two-Color X-Ray Free-Electron Lasers

A.A. Lutman<sup>1</sup>, R. Coffee<sup>1</sup>, Y. Ding<sup>1</sup>, Z. Huang<sup>1</sup>, J. Krzywinski<sup>1</sup>, T. Maxwell<sup>1</sup>,  
M. Messerschmidt<sup>1</sup>, H.-D. Nuhn<sup>1</sup>

<sup>1</sup> SLAC National Accelerator Laboratory, Menlo Park, CA 94025, USA

## Abstract

With an eye toward extending optical wave-mixing techniques to the x-ray regime, we present the first experimental demonstration of a two-color x-ray free-electron laser at the Linac Coherent Light Source (LCLS). We combine the emittance-spoiler technique with a magnetic chicane in the undulator section to control the pulse duration and relative delay between two intense x-ray pulses and we use differently tuned canted pole undulators such that the two pulses have different wavelengths as well. Two schemes are shown to produce two-color soft x-ray pulses with a wavelength separation up to  $\sim 1.9\%$  and a controllable relative delay up to 40 femtoseconds.

*Phys. Rev. Lett.* 110, 134801 (2013)

Work supported by Department of Energy contract DE-AC02-76SF00515.

The rapid development of x-ray free electron laser (FEL) techniques is fueling a revolution in chemical and materials dynamics. The recent advent of sub-10 femtoseconds (fs) x-ray pulses raises the possibility for pump-probe techniques as are common in the optical regime that often use two different color excitations. The prospect of multi-wave mixing in the x-ray regime has therefore motivated us to pursue two-color double x-ray pulses with controllable relative delay and color separation. With this two-color feature in the x-ray regime one can follow both chemical reactions and electronic evolution in materials on their natural time scales. Further, ultrafast chemical and materials dynamics are driven largely by valence and inter-band transient excitations on the order of a few eV. Based on the current hardware configuration of the LCLS we demonstrated a controllable delay of 0 – 40 fs and a color separation of up to  $\sim 30$  eV at 1500 eV. This result fits perfectly into the material and chemical natural time and energy scales and is sure to enable numerous experimental techniques in the years to come.

Time-domain spectroscopy capitalizes on the interplay between the conjugate variables of frequency and time. Measuring the temporal evolution of, e. g., optical absorption, one can discover the coupling between different modes of internal molecular motion [1]. A similar approach in the x-ray regime has recently been proposed as a spectroscopic technique for measuring ultrafast charge transfer in molecules [2]. The time scale for such dynamics can be as fast as 10 fs as in dissociative ionization [3] or in the 25–50 fs regime for less energetic chemical mechanisms such as hydrogen elimination from ethylene [4, 5]. Photochemistry in the visible to ultraviolet regime could then be explored with color separations within 10 eV and inter-pulse delays in the 10–50 fs range.

In condensed phase, typical final exciton energies associated with carrier-carrier scattering are on the order of the 5–10 eV. One might imagine stimulated resonant inelastic x-ray scattering techniques as a probe of the occupancy of these transient excitonic states. As an example, recent calculations point to an anisotropy in the optical carrier-hole excitation in graphene that quench with  $\sim 10$  fs-scale dynamics [6]. Rapid bulk thermalization of coherent excitation is sure to continue occupying the scientific landscape into the foreseeable future. This could be another avenue enabled by the time and energy separations accessible in the two-color schemes presented here.

Two-color FEL operation was first reported in 1994 for a low-gain, infrared oscillator FEL configuration [7], where a single electron beam and two undulator sections were used.

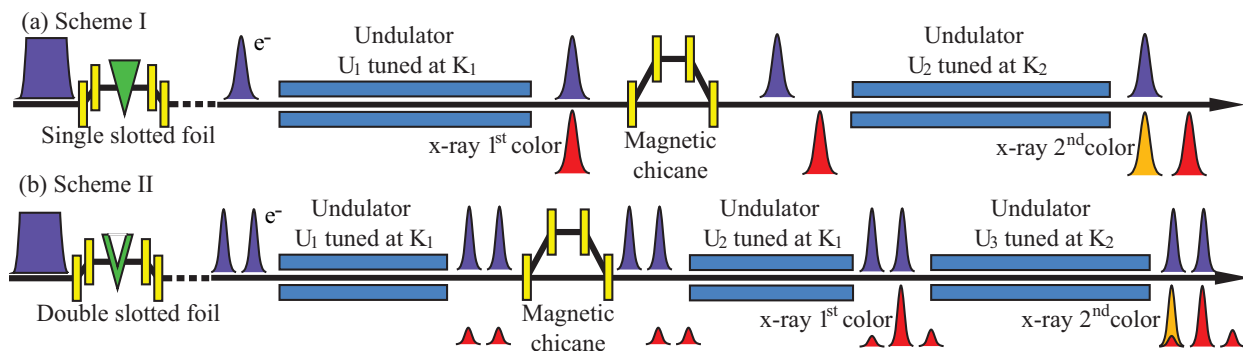


FIG. 1. Two-color FEL schemes tested at the LCLS. A single-slot (in scheme-I) or double-slot (in scheme-II) emittance spoiling foil was used to generate ultrashort single or double electron bunches. The emittance-spoiling foil is located in the second bunch compressor.

A magnetic chicane, designed for hard x-ray selfseeding purpose, was adopted here to control the temporal delay between the two-color pulses.

Another two-color FEL experiment, also in the low-gain, long wavelength regime, was based on a pulse switching method at a superconducting accelerator [8]. Recently, rapid progress in high-gain FEL motivated several proposals to create two-color FELs in the x-ray wavelength regime [9–15]. To the best of our knowledge, two-color x-ray FELs have not been demonstrated anywhere in the past. This paper reports the first experimental demonstration of two-color x-ray FEL operation based on two different schemes to be described in the following.

At the LCLS, one can tune the final x-ray wavelength by adjusting either the electron beam energy or the undulator strength; a flexibility that has enabled our demonstration of fully tunable two-color operation. In an FEL, it produces a high intensity, narrow bandwidth radiation around the resonant wavelength  $\lambda_r$ ,

$$\lambda_r = \frac{\lambda_u}{2\gamma^2} \left( 1 + \frac{K^2}{2} \right), \quad (1)$$

where  $\gamma$  is the Lorentz factor,  $\lambda_u$  is the undulator period and  $K$  is the dimensionless undulator strength parameter. The LCLS is based on planar, permanent-magnet undulators with a fixed gap but the magnet poles have canted angles [16]. This feature allows for tuning  $K$  in a range between roughly 3.47 to 3.51. Used routinely to taper the undulator strength, the canted poles were adjusted in this study to produce FEL lasing at two distinct soft x-ray wavelengths. In addition, the 16th of the 33 undulator sections was recently replaced with

a 3.2 m-long magnetic chicane for the hard x-ray self-seeding program [17]. In self-seeding this magnetic chicane delays the electron bunch relative to the x-rays and washes out the microbunching generated in the first undulator section. Our two-color FEL scheme uses this same function to produce the delay-tunable two-colors, but in SASE mode rather than seeded.

For this study, we combined the canted pole undulators, the seeding chicane, and the emittance-spoiling foil to demonstrate full control of the pulse duration, relative delay, and spectral separation as the first experimental study of two schemes for two-color soft x-ray FEL operation at LCLS. The two schemes are depicted in Fig. 1. Simulation studies were reported previously for similar schemes in Ref. [15]. Both two-color schemes used the LCLS in the soft x-ray regime at 1.5 keV with an emittance-spoiling foil [18] to control the electron bunch duration (Scheme I) or to produce two bunches with a variable delay (Scheme II) [19]. The emittance-spoiling foil is located in the second bunch compressor. The undulator period was 3 cm and the electron beam energy was set to 5.8 GeV. Each undulator’s magnetic length was 3.3 m and a linear taper in  $K$  for each section compensated for electron beam energy loss due to spontaneous emission and wakefields. For each machine setting, a series of roughly 25,000 single-shot spectra were recorded with the single-shot soft x-ray spectrometer described in Ref. [20] using the 100 lines/mm gratings.

Under scheme I, Fig. 1a, the electron bunch passed through a single-slot emittance spoiler. In our test, the spoiler was set to pass a single unspoiled electron bunch that corresponded to about 18 fs FWHM in duration. The expected x-ray pulse duration is similar or shorter [19, 21]. The pulse duration can be controlled by choosing the slot width (a triangularly shaped slot) to satisfy different experimental requirements. The peak current was set to 1.6 kA. An x-ray pulse was generated at wavelength  $\lambda_1$  in the first undulator section,  $U_1$ , that was tuned to a strength parameter  $K_1 = 3.481$ . The 9 undulators that comprised  $U_1$  were chosen to yield an intense FEL pulse while avoiding saturation. The energy spread developed by the electron beam in  $U_1$  was therefore small enough to preserve the electron beam for effective lasing in the subsequent section. The magnetic chicane between the two undulator sections delayed the electron beam relative to the photon beam and also washed out the microbunching that developed in  $U_1$ . Set to zero deflection, the chicane (it is a drift actually) produced a minimal delay between the two pulses,  $\tau_{\text{min.}} = l/v_{\text{drift}} - l/c$ , where  $c$  is the speed of light,  $l \sim 4$  m is the length between undulator sections, and  $v_{\text{drift}}$  is the

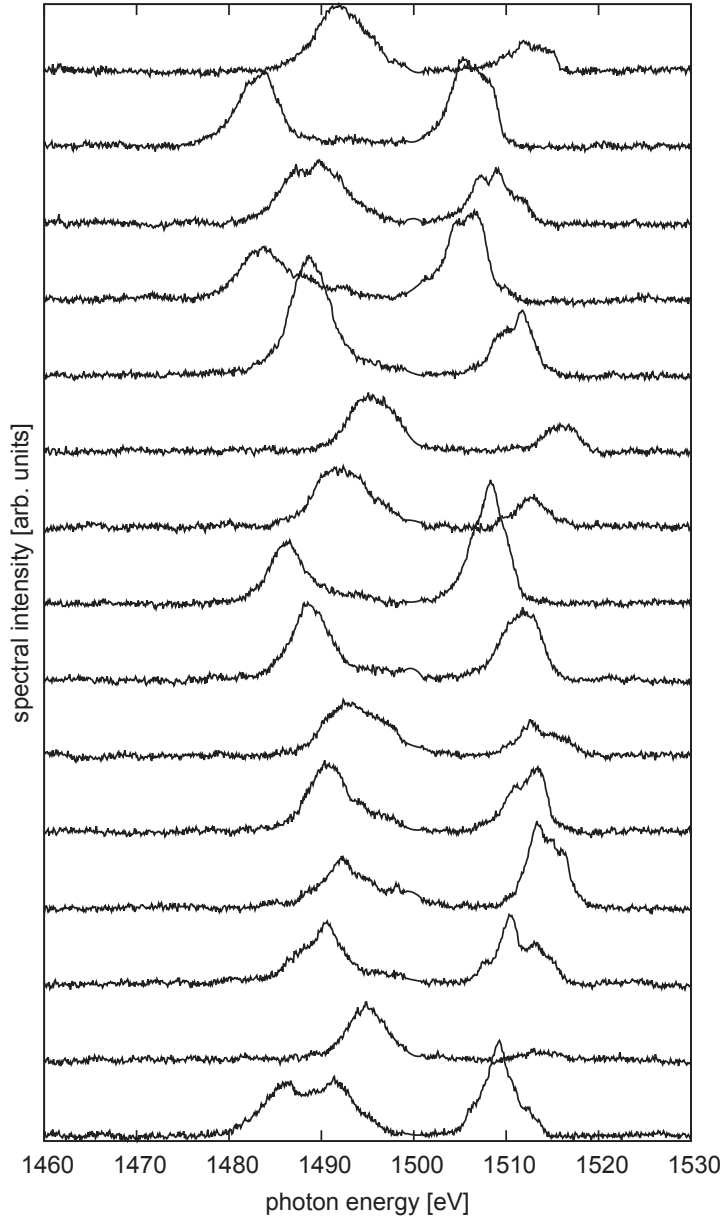


FIG. 2. Fifteen consecutive x-ray spectra produced under scheme I with chicane delay set to the nominal 0 fs.

drift velocity of the electron bunch. This drift mismatch is typically in the range of tens of attoseconds and so we refer to this minimal delay as 0 fs. Although the maximum delay could be as long as 40 fs, the chicane was used to produce a maximum of 25 fs of delay for this study. The second 10 undulator long section,  $U_2$ , was tuned to a strength parameter  $K_2 = 3.504$ , to produce a second x-ray pulse at the wavelength  $\lambda_2$ .

A sequence of 15 consecutive shots, displayed in Fig. 2 show that the majority of the shots

produce two spectrally separated pulses. Common to the SASE process, the individual pulses show multi-mode spectral structure that is a bit too fine for the spectrometer resolution. The shot-to-shot energy jitter does not affect the energy separation and so the electron beam energy fluctuations can be sorted in post-analysis to yield the linear dependence of photon energy on electron beam energy. This linear dependence is evident in Fig. 3a and b where the results have been averaged, peak-normalized for each electron beam energy, and sorted accordingly for 0 fs and 25 fs delays, respectively. We note that plotted this way, we can identify only very slight systematic variation of the relative peak shapes versus photon energy. The spectra are subsequently realigned based on the correlation, averaged, and shown in Fig. 3c and d.

The energy-aligned spectra show an average energy difference between the two pulses of 20 eV or 1.3% of the mean photon energy with the earlier described undulator configuration. In the case of the nominal 0 fs chicane delay (Fig. 3a & c), the mean for the total x-ray pulse energy is 100  $\mu\text{J}$  with the higher photon energy produced in  $U_1$  containing about 40  $\mu\text{J}$  of the total energy in 5.5 eV FWHM bandwidth and the remaining 60  $\mu\text{J}$  of energy within 8.2 eV FWHM bandwidth from  $U_2$ . In the case of 25 fs chicane delay (Fig. 3c & d), the peak current was changed to 1.4 kA in order to balance the intensities of the two colors and the mean total energy was 45  $\mu\text{J}$ , less than half of the 0 fs case. The higher frequency pulse contained about 20  $\mu\text{J}$  in a 6.5 eV FWHM bandwidth and the lower frequency pulse contained about 25  $\mu\text{J}$  in a 7.7 eV FWHM bandwidth. To study the correlation between the two colors, each collected spectrum was fit with a sum of two Gaussians, and the energy of each color measured as proportional to the area of its Gaussian fit. Figures 5a and b show the shot-to-shot correlation between the two colors for the scheme I. The fluctuations for the first color, calculated as the ratio between the standard deviation and the average of the energy, are of 60% for the first color and 27% for the second color in the 0 fs delay case, and 65% of and 32% for the 25 fs delay case.

We achieved the maximum color separation of  $\sim 1.9\%$  when we maximized the difference of the two strengths ( $K_1$  and  $K_2$ ) in the undulator setup, within the present LCLS undulator strength range.

Scheme II, shown in Fig. 1b, uses three undulator sections and is closely related to that proposed in Ref. [10]. The parent electron bunch was passed through a double-slotted, emittance-spoiling foil. The two  $\sim 10$  fs-long unspoiled bunches contained nearly equal cur-

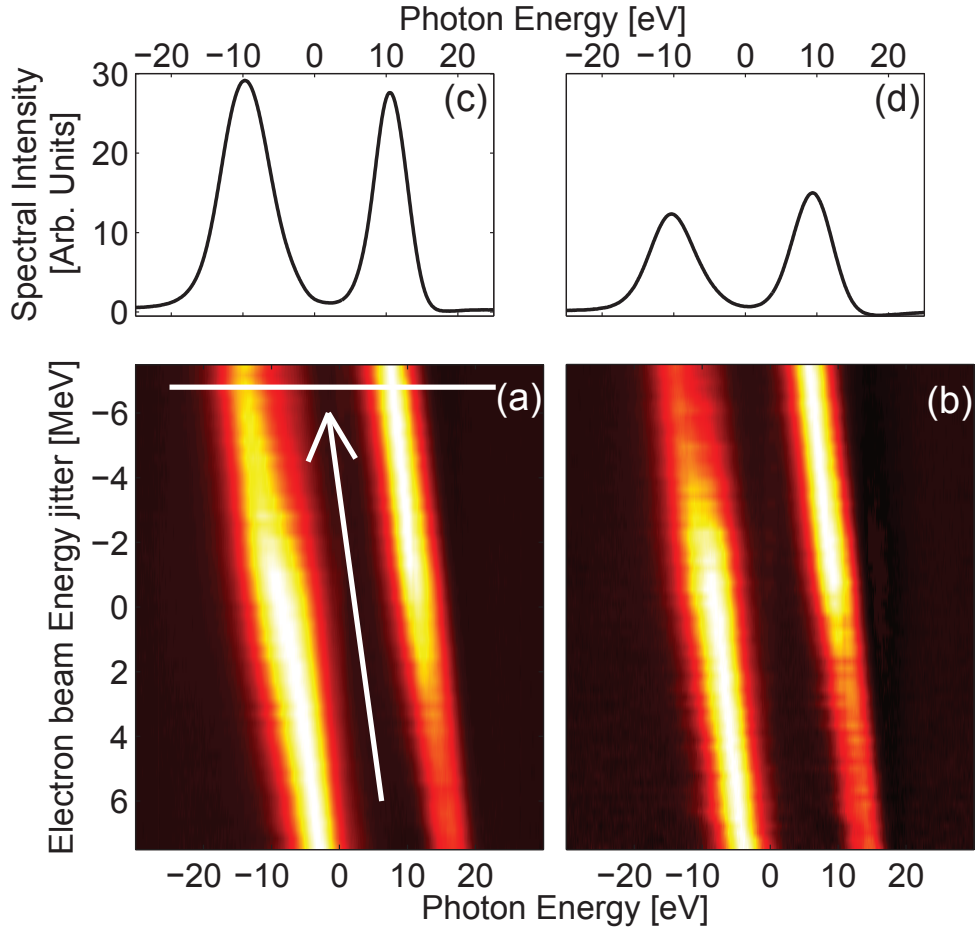


FIG. 3. Results for two-color beams with scheme I. (a,b) Average spectral intensity as function of the electron beam energy and photon energy. For each electron beam energy, the maximum intensity has been normalized to 1. (a) 0 fs delay. (b) 25 fs delay. (c,d) Average realigned spectra as a function of the photon energy offset from 1.5 keV. (c) 0 fs delay. (d) 25 fs delay.

rent and electron beam energy. Two longitudinal separations were chosen to give 21 fs and 26 fs inter-pulse separations in our study. The peak current was set to 1.5 kA. Ten undulators were used for  $U_1$  in order to keep the FEL intensity for each bunch well below saturation. The section  $U_1$  was tuned to  $K_1 = 3.483$  to produce a wavelength  $\lambda_1$ . After exiting  $U_1$ , the magnetic chicane established temporal overlap between the trailing x-ray pulse and the unspoiled part of the leading electron bunch. This overlap was achieved by a cross-correlation measurement as reported separately in [19]. This chicane also washed out the microbunching that was produced in the  $U_1$  section. The second undulator section  $U_2$  was tuned also to  $K_1$  and consisted of 5 undulators. In  $U_2$  the trailing x-ray pulse overlapped

a fresh portion of the leading electron bunch, thus seeding the bunch in order to reach saturation at  $\lambda_1$ . The 12 undulator-long section  $U_3$  was tuned to  $K_2 = 3.501$ . In  $U_3$  the trailing bunch reached saturation at the wavelength  $\lambda_2$  but the lasing of the leading electron bunch was suppressed since it had developed too large of an energy spread in  $U_2$  to lase well in  $U_3$ .

Figure 4a and b show the spectral intensity as a function of the photon energy and electron beam energy for the 21 fs and 26 fs delay cases, respectively. As in scheme I, the two colors are well separated, this time by about 15 eV, and exhibit the usual linear correlation between photon energy to electron beam energy. Realigning the spectra as before (not shown), the average pulse energies (FWHM bandwidths) were measured for the 21 fs case to be 10.5  $\mu\text{J}$  (4.5 eV) and 7.1  $\mu\text{J}$  (7.6 eV) for the higher and lower frequency photon beams, respectively. In the 26 fs case, the average energies (bandwidths) were 11.1  $\mu\text{J}$  (4.5 eV) and 7.6  $\mu\text{J}$  (8.0 eV) for the higher and lower frequency pulses respectively. Figures 5c and d show the shot-to-shot correlation between the two color energies; for both sets, the fluctuations for the first color are of  $\sim 75\%$ , while the fluctuations for the second color are of  $\sim 55\%$ . Numerical simulations predict that both pulses should reach saturation when the setup for scheme II is tuned properly[15], in our experiment the fluctuations for the second scheme were still large indicating that a better tuning was needed to reach saturation for both colors.

Comparing the two schemes, we can identify specific merits and disadvantages for each two-color technique. The second scheme requires a delicate balance of three undulator sections and the double-slotted foil. From Figs. 3 and 4 there seems to be a stronger systematic variation of the relative peak shapes versus photon energy for scheme II compared to scheme I, although scheme II may be further optimized. Scheme II is unable to achieve the temporal overlap and on the other hand it can only produce delays over the central flat length of the parent electron bunch. Unlike scheme II, however, scheme I cannot achieve saturation in the first x-ray pulse and therefore will exhibit a stronger shot-to-shot relative intensity fluctuation for the two colors. Nevertheless, scheme I can achieve a partial temporal overlap between the pulses, within the delay due to the difference between the electron bunch velocity and the group velocity of the FEL pulse. The delay is about  $N\lambda_r/c$ , being  $N$  the number of undulator periods in a single undulator section and is estimated about 3 fs based on the FEL parameters presented here. The presented schemes have been demonstrated in the soft x-rays but are applicable also for the hard x-rays. The described delay between the pulses is proportional to the wavelength, thus the use of hard x-rays would improve the



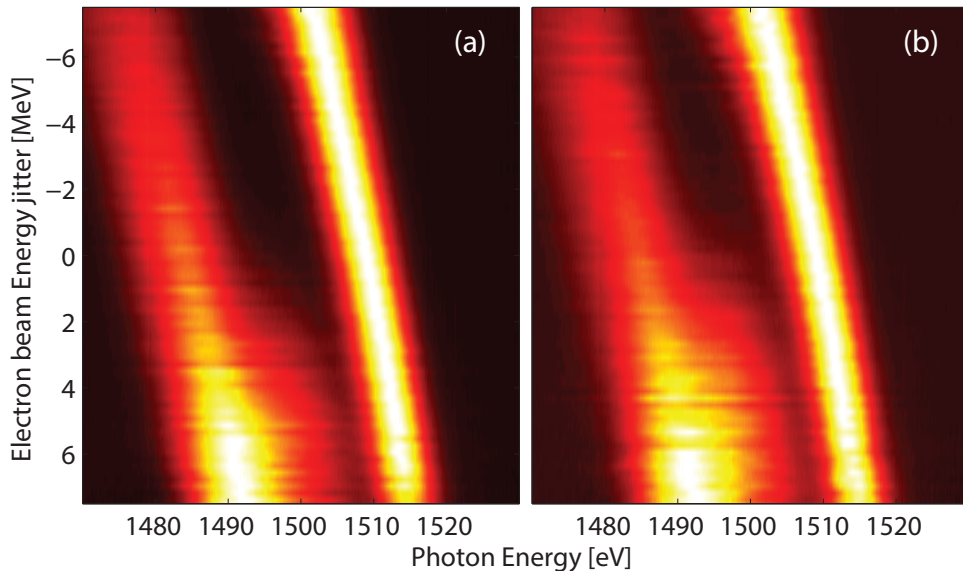


FIG. 4. Results for two-color beams with scheme II. (a,b) Average spectral intensity as a function of the electron beam energy and photon energy. For each electron beam energy, the maximum intensity has been normalized to 1. (a) 21 fs delay. (b) 26 fs delay.

achievable overlap between the pulses. Since we use the same electron bunch to generate two-color pulses, the timing jitter between them is only introduced in the chicane by the electron beam energy jitter and the chicane dipole magnetic field jitter. Each contribution is less than 0.2% of the delay imposed by the chicane. This timing jitter is negligible, even compared with an extremely short 1-2 femtosecond pulse. Scheme I can also be used in conjunction with either spoiler control of the pulse duration or with the low-charge operation mode [22] to generate short pulses.

We have shown two schemes that produce delay-controllable x-ray pulses with relative delays of up to 40 fs and energy separations that are also controllable up to  $\sim 1.9\%$  of the central energy at LCLS. Note that once a variable-gap undulator is used, the energy separation of the two colors can be largely increased. And the present maximum delay of 40 fs in our study is determined by the small chicane which was designed for LCLS self-seeding purpose. A specific chicane to provide a much larger delay can be designed for future facilities. Also an optical delay line for the first color x-rays can be added so that it provides a flexible control of the delay between the two colors, realizing a full overlap or even cross-over. This ability to operate an x-ray FEL with two pulses with controllable

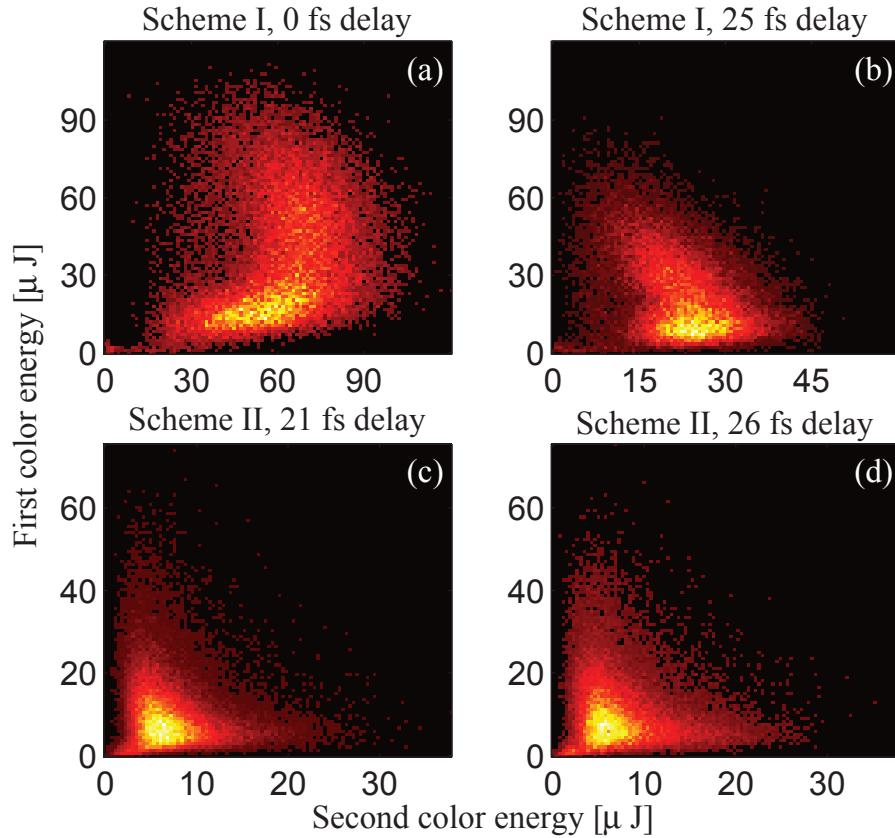


FIG. 5. Shot-to-shot intensity correlation between first and second color generated in the Two-Color schemes. Each spectrum has been fit with a sum of two Gaussians, and the energy is considered proportional to the fit area. (a) Scheme I with 0 fs delay, (b) Scheme I with 25 fs delay, (c) Scheme II with 21 fs delay, (d) Scheme II with 26 fs delay.

wavelength separation that can be delayed from coincidence to  $\sim 40$  fs is of extreme value to the future of time-domain x-ray spectroscopy.

We thank J. Arthur, H. Durr, C. Feng, W. Fawley, W. Schlotter, J.J. Turner and J. Wu for useful discussions and support, and also thank the operation group for their dedicated support. This work was supported by DOE contract DE-AC02-76SF00515.

- 
- [1] J. F. Cahoon, K. R. Sawyer, J. P. Schlegel, and C. B. Harris, *Science* **319**, 1820 (2008).
  - [2] J. D. Biggs, Y. Zhang, D. Healton, and S. Mukamel, *J. Chem. Phys.* **136**, 174117 (2012).
  - [3] I. A. Bocharova, A. S. Alnaser, U. Thumm, T. Niederhausen, D. Ray, C. L. Cocke, and I. V.

- Litvinyuk, *Physical Review A* **83**, 013417 (2011).
- [4] H. Tao, T. K. Allison, T. W. Wright, A. M. Stooke, C. Khurmi, J. van Tilborg, Y. Liu, R. W. Falcone, A. Belkacem, and T. J. Martinez, *J. Chem. Phys.* **134**, 244306 (2011).
- [5] T. K. Allison, H. Tao, W. J. Glover, T. W. Wright, A. M. Stooke, C. Khurmi, J. van Tilborg, Y. Liu, R. W. Falcone, T. J. Martinez, and A. Belkacem, *J. Chem. Phys.* **136**, 124317 (2012).
- [6] T. Winzer, A. Knorr, M. Mittendorff, S. Winnerl, M.-B. Lien, D. Sun, T. B. Norris, M. Helm, and E. Malic, *App. Phys. Lett.* **101**, 221115 (2012).
- [7] D. A. Jaroszynski, R. Prazeres, F. Glotin, and J. M. Ortega, *Physical Review Letters* **72**, 2387 (1994).
- [8] T. Smith, E. Crosson, G. James, H. Schwettman, and R. Swent, *Nucl. Instr. and Meth. A* **407**, 151 (1998).
- [9] H. P. Freund and P. G. O'Shea, *Physical Review Letters* **84**, 2861 (2000).
- [10] G. Geloni, V. Kocharyan, and E. Saldin, Report No. DESY-10-004, (2010).
- [11] G. Geloni, V. Kocharyan, and E. Saldin, Report No. DESY-10-006, (2010).
- [12] A. Zholents and G. Penn, *Nucl. Instr. and Meth. A* **612**, 254 (2010).
- [13] A. Zholents, NGLS Technical Note No.25 (2012).
- [14] G. Geloni, V. Kocharyan, and E. Saldin, *Optics Communications* **284**, 3348 (2011).
- [15] C. Feng *et al.*, in Proceedings of the 34th Free Electron Laser Conference, Nara, Japan, August 2012.
- [16] P. Emma *et al.*, *Nat. Photon.* **4**, 641 (2009).
- [17] J. Amman *et al.*, *Nat. Photon.* **6**, 693 (2012).
- [18] P. Emma, K. Bane, M. Cornacchia, Z. Huang, H. Schlarb, G. Stupakov, and D. Walz, *Physical Review Letters* **92**, 074801 (2004).
- [19] Y. Ding *et al.*, *Physical Review Letters* **109**, 254802 (2012).
- [20] P. Heimann *et al.*, *Rev. Sci. Instrum.* **82**, 093104 (2011).
- [21] A. A. Lutman, Y. Ding, Y. Feng, Z. Huang, M. Messerschmidt, J. Wu, and J. Krzywinski, *Phys. Rev. ST Accel. Beams* **15**, 030705 (2012).
- [22] Y. Ding *et al.*, *Physical Review Letters* **102**, 254801 (2009).